The Role of Local Heating in Producing Temperature Variations in the Offshore Waters of the Eastern Tropical Pacific

ANTS LEETMAA

Atlantic Oceanographic and Meteorological Laboratories, NOAA, Miami, FL 33149

(Manuscript received 12 July 1982, in final form 22 November 1982)

ABSTRACT

The role of local heating in producing annual and interannual sea-surface temperature variations in the eastern tropical Pacific is studied. Removed from the eastern boundary (122°W), and off the equator, local heating plays a major role in producing annual temperature fluctuations. At the same longitudes from 10°N to 10°S interannual variations in the yearly-average temperature and the anomalous net heat input into the ocean are of the same sign and magnitude. During the 1969 and 1972 ocean warmings there was increased heat input into the ocean. Closer to the eastern boundary, oceanic processes such as advection are as important as local heating. Results from a simple model incorporating local heating, offshore Ekman transports, and upwelling suggest the following scenario for the 1972–73 El Niño. During February and March 1972 enhanced local heating and reduced offshore advection were the main reasons for anomalously warm temperatures in the open ocean adjacent to Peruvian coastal waters. From April 1972 to March 1973 temperatures remained high because of offshore transport of anomalously warm inshore waters. Whether the latter were warm because of upwelling of warmer water or transport of warmer water from farther south is not clear.

1. Introduction

The eastern equatorial Pacific is a region of positive heat gain from the atmosphere. Studies show that along the equator and south of the equator along the coast of South America the yearly average heat input is greater than 100 W m^{-2} (Weare, *et al.*, 1981). If this heat were evenly distributed over the top 40 m of the ocean, which is approximately the mixed layer depth in this region, the ocean would heat up at the rate of 1.5°C per month. Observed monthly temperature changes are comparable to this during the heating season. However, on the yearly average, oceanic processes must remove heat from this area.

This region is also one in which there are large interannual variations in the sea-surface temperature (SST). Locally, these are known as El Niño events. The time and space evolution of the warm anomalies has recently been described by Rasmusson and Carpenter (1982). When they are fully developed, they encompass almost the entire equatorial Pacific. Recent theoretical studies have shown that it is at this time that they seem to influence the atmospheric circulation patterns so as to modify mid-latitude weather (Horel and Wallace, 1981; Hoskins and Karoly, 1981). The amplitude of the positive anomalies in the eastern Pacific is 2–4°C. This is comparable to the amplitude of the annual temperature cycle in this region.

A number of different mechanisms have been proposed as being responsible for El Niños. Bjerknes (1966) and Wyrtki (1975) suggested that an important factor in these events is the adjustment of the equatorial current systems to variations in the strength of the trades far removed from the eastern boundary. A number of recent theoretical studies have modeled the response of the upper layer thickness of the ocean to changes in the large-scale wind fields (McCreary, 1976; Busalacchi and O'Brien, 1981). The latter study has achieved remarkable success in simulating observed upper-layer thickness variations in the eastern Pacific using observed wind-stress fields. With the exception of McCreary (1976), little theoretical work has been done to model the observed southward cross-equatorial flooding of warm low-salinity water. Observations indicate that this process happens during every major El Niño.

Previous work has not considered the role of local heating in producing anomalously warm temperatures. Considering the large mean heating rates, it would be surprising if variation in local heating or in the processes that export this heat were not important. In this paper the importance of local heating in producing annual and interannual temperature variations is studied. The annual cycle is examined because its amplitude is large in the far eastern Pacific. Hence, the mechanisms that produce these temperature variations are vigorous and perhaps may be more easily understood than the rarer El Niño events. Second, the maximum anomalies during El Niños occur at the same time as peak temperatures during the annual cycle. Possibly, the former represent an

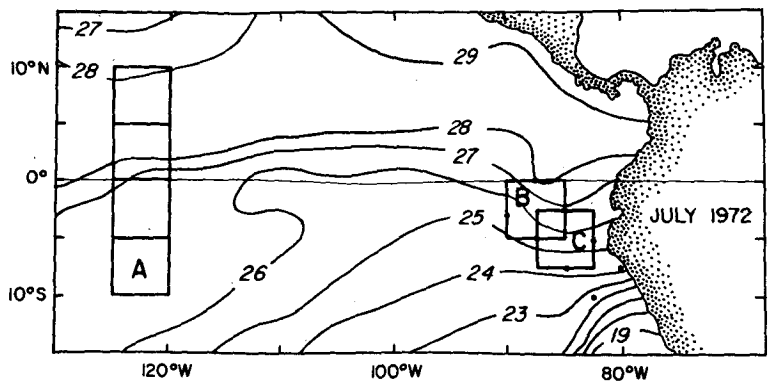

FIG. 1. Surface temperature for July 1972, from Ramage *et al.* (1980). The squares are regions where heat computations were performed.

extreme manifestation of the latter. Finally, interannual variations in the heating are studied to see if these could cause interannual variations in the SST.

Several data sources were used. Historical monthly-mean values of the wind, sea temperature, wet bulb, dew point, and air–sea temperature difference were obtained from the National Climatic Center for the locations shown in Fig. 1. Cloudiness data for 1966–73 were obtained from the cloud atlas of Sadler, *et al.* (1976). For the 1972–73 El Niño monthly values of the winds, sea-surface temperature (SST) and the net heat gain were available from Ramage *et al.* (1980). Standard bulk formulas were used to compute the terms in the heat budget from the monthly-mean data. These formulas are described in the Appendix.

2. The annual cycle

A simple ocean mixed-layer model is used which ignores all horizontal and vertical mixing and advection. The heat that is put into the ocean is assumed to be mixed uniformly over the top 40 m. This is approximately the depth to which annual heating is confined. Hence surface and mixed-layer temperature changes are given by $\partial T/\partial t = (1/\rho C_p H)Q$; Q is the heat input, H the depth of the mixed layer, ρ the density of seawater, C_p the heat capacity at constant pressure. This model presumably is too simple. However, the goal is not to simulate exactly the SST variations but rather to see if their amplitude and phase can be reasonably accounted for. Other effects such as advection and mixed layer deepening probably are important at times. The present model is used primarily to explore when, and if, local effects are dominant.

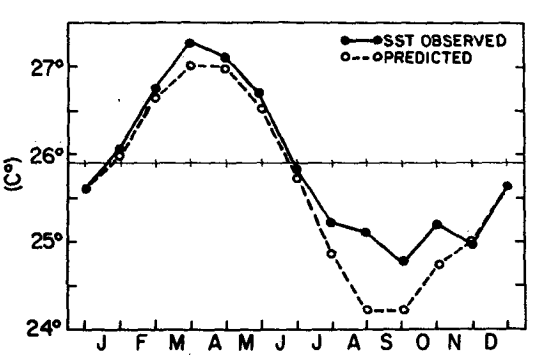

FIG. 2. Annual temperature cycle in Area A.

The results for Area A (Fig. 1) are shown in Fig. 2. This region was picked to lie far enough off the equator and offshore such that horizontal gradients of temperature and hence advective effects would not dominate. On the other hand, Areas B and C were picked such that these effects probably would be important. As can be seen, there is reasonable agreement in Region A between the observed temperature changes and those caused by local heating. A discrepancy occurs in July–September when the ocean does not cool off so much as is predicted by the model. This could be caused by advective effects or a deepening of the mixed layer. This latter effect is observed to occur at about this time (Wyrtki, 1964). Overall, however, the phases and amplitudes of the two curves are in reasonable agreement. This suggests that local heating is very important for the annual cycle in this region. The mean heating rate has been removed for this computation.

Local heating is not nearly so dominant in Area B. Instead of showing the annual temperature-variation curves, the heating rates (°C per month) are shown in Fig. 3. The ocean is observed to start cooling in April, whereas positive heat input occurs through May. Similarly, observed heating starts in September whereas the net heating curve doesn't show a positive gain until December. Here again the mean heating has been removed. From the phase differences, it is clear that oceanic effects such as advection must be very important. What these effects are is open to speculation. Historical observations suggest that the cooling in April is a combination of a northward movement of the equatorial front which frequently is found

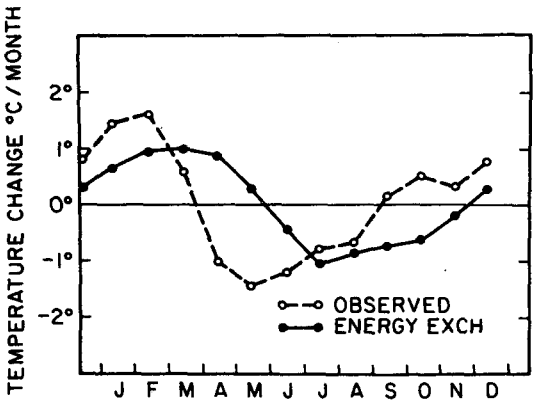

FIG. 3. The annual cycle of temperature change per month in Area B. The large difference between these curves suggests the ocean plays an important role in the heat budget in this region.

south of the equator early in the year, and the offshore advection of cooler upwelled water. More puzzling is the reason for the heating during the second half of the year since during this time the winds are still favorable for upwelling.

3. Interannual variations

These model computations were performed to see if interannual variations in local heating and SST variations could be related. Previous work had suggested that in Area A, year-to-year variations in the yearly-mean temperature were related to net local heat changes (Dewitt, 1979). Since this manuscript is unpublished, the relevant figure is reproduced here (Fig. 4). That computation differed only from these in that the heat was distributed over a triangular shape in the vertical (of maximum width at the surface and zero width in the middle of the thermocline). The temperature in this triangular area was still assumed to be uniform. The depth of the middle of the thermocline was approximately 100 m at 7.5°N, 2.5°N, and 2.5°S and 150 m at 7.5°S. If the heat were mixed uniformly with depth instead, the effective mixed-layer depth would be about one-half of these thermocline depths. The mean heating for the period 1966–72 was removed. Again there is reasonable agreement between the observed and predicted changes (Fig. 4). The El Niños of 1969 and 1972 occurred during years in which the heat input to the ocean was greater than average. Similarly, the cool years of 1970 and 1971 coincided with a weaker-than-average heat input. These results hold for all four of the 5° squares. Hence, they probably are not a result of an inadequate data base. The cooling in 1971 and 1972 in this calculation seems to have resulted primarily from reduced evaporation. The warming in 1972 resulted from reduced evaporation during the first part of the year and an increase in the incoming radiation during the second half. Thus, it seems that far removed from the eastern boundary, local heating

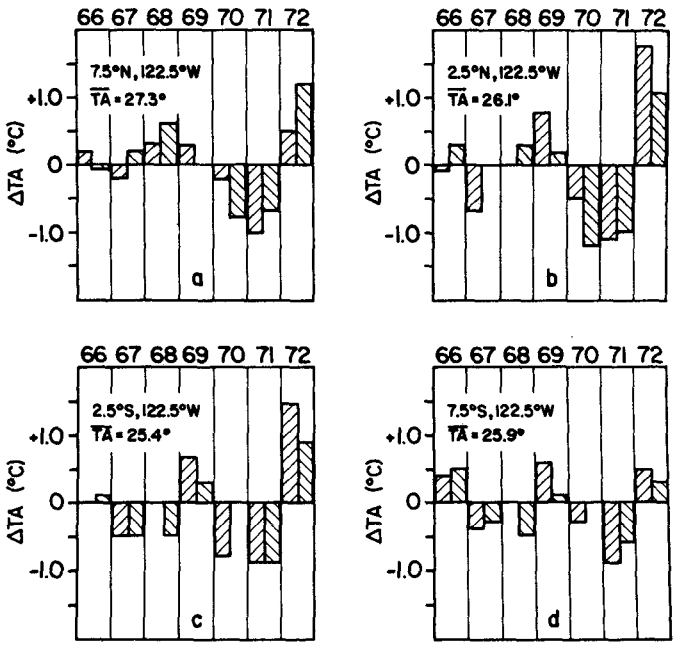

FIG. 4. Comparisons between the observed and computed yearly-mean temperatures along 122.5°W from 10°N to 10°S. The observed values are indicated by shading in which the lines run from lower left to upper right. The model values have the stripping running from upper left to lower right.

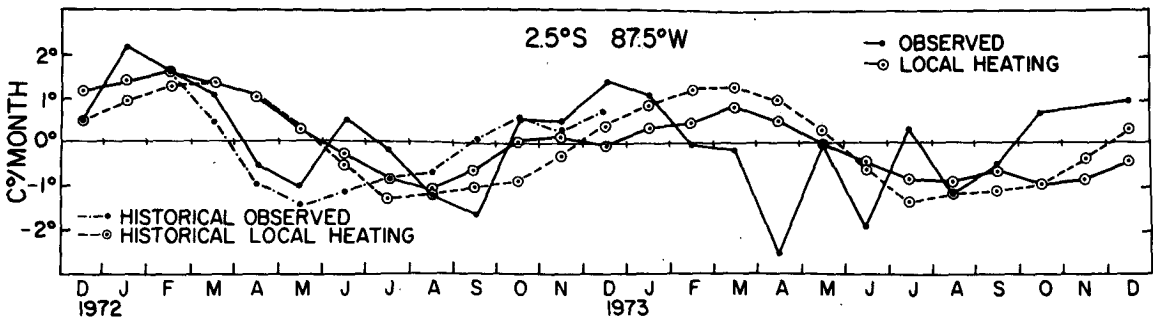

FIG. 5. The monthly cycle of temperature change per month for 1972–73 in Area B. Historical data was obtained from National Climatic Center. Historical heating computed for years 1966–72.

is also important in causing interannual variations in oceanic temperatures.

Using the monthly net heating values (with the 1972–73 mean removed) from Ramage *et al.* (1980), the monthly-average temperature changes were computed for Region B for 1972 and 1973. These are compared with the observed rates in Fig. 5. Since the annual cycle has not been removed, there is a great deal of similarity between these results and the mean-monthly changes shown in Fig. 3. As in the annual case, the ocean starts cooling early in the year while local heating was still putting heat into the ocean. Similarly, in both years the ocean was observed to start heating in October at a greater rate than the local heating or while the latter was still cooling. There is also an observed heating in June of 1972 which is not reflected in the computed curve.

Compared to the 1966–72 average-monthly values, both the observed and computed heating rates were greater in 1972 than the average ones. The anomalous heating in late 1971 and early 1972 was a result of reduced evaporation and reduced cloudiness. During the latter half of 1972 it resulted primarily from an increase in the incoming radiation. This was deduced by comparing the terms in the heat budget for late 1971 and 1972 with those for 1973, using the atlas of Ramage *et al.* (1980). The anomalous heating in late 1971 and 1972 is ~50% greater than the mean. [This presumes, of course, that our mean-monthly 1966–72 rates are representative of longer term mean rates and that our bulk formulas give comparable results to those of Ramage *et al.* (1980) with the same data.] The observed net heating in 1972, which is the sum of the individual monthly rates, was observed to be 3.1°C whereas the computed excess was 1.7°C. In 1973 these values were −2.3°C and −1.7°C, respectively. These results are consistent with those shown in Fig. 4. During the El Niño year there was a greater than average input of heat into the ocean.

4. A model including the mean heating

A shortcoming of the previous computations is that the mean heating rates have been ignored. It is assumed that somehow this heat is removed by a mean circulation. This mean heating amounts to a temperature increase of ~1.5°C per month. If during anomalous years the circulation patterns are significantly altered because of changes in the local winds or remotely forced effects, the previously presented computations could be significantly altered. Maps of the surface temperature distribution in this region (Fig. 1) suggest that offshore and westward advection is a major mechanism by which heat is removed from this area.

To see if inclusion of upwelling and offshore wind drift improves our understanding of the mechanisms that produce SST variations, the following simple model is considered. From the atlas of Ramage *et al.* (1980), the monthly-mean SST, wind stress, and net heating were computed in region C, that is, the 5°-square centered at 5°S, 85°W. This lies just offshore of the coastal upwelling regime. The equation $\rho h C_p(\partial T/\partial t + u\partial T/\partial x) = Q$ is solved in this square where x is the offshore direction. It is again assumed that the heat and momentum are uniformly mixed over 40 m. The offshore velocity u is the average Ekman velocity, which is determined from $\tau/\rho Hf$. Average values for Q, T, τ were determined from the four grid points on the periphery of this square (Fig. 6). Monthly values for the inflow temperature T_0 were determined by adding one degree to the average monthly temperature at the points 7.5°S, 80°W, 10°S, 82.5°W. The atlas shows that the water heats up by a degree or so from these grid points to the boundaries of the square. The geometry and method of solution are schematically shown in Fig. 6. Any parcel starting at the right hand side of the square heats up as it moves westward at the rate $dT/dt = (\rho C_p h)^{-1}Q$. Thus, after one month its temperature has increased by $\Delta T = (\rho C_p h)^{-1}Q \times 1$ month. The distance it has moved to the west is $\Delta x = \tau/\rho hf \times 1$ month because of Ekman advection. Its temperature after one month is $T_1 = T_0 + \Delta T$. To the east of this position the temperature varies linearly from T_1 to T_0. To the west of Δx, the temperature at any point x is given by $\Delta T + T_p(x - \Delta x)$ where T_p is the

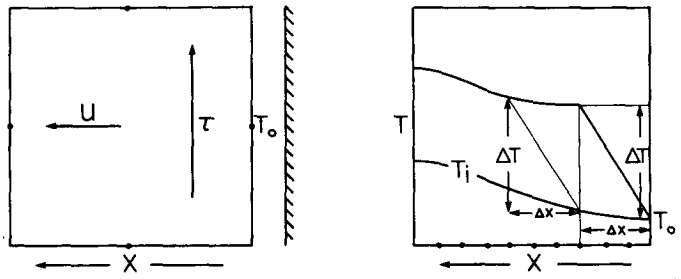

FIG. 6. Left panel shows model geometry. Observed data were available at points on sides of square. See text for discussion of how T_0 was determined. Right panel schematically shows method of solution.

temperature at grid point $x - \Delta x$ at the end of the previous month.

Starting with a constant temperature of 18.7°C across the whole box in November 1971, the above procedure was followed for each month from December 1971 to December 1973. In late 1971, the magnitude of the offshore Ekman flux was such that it took 3–4 months for a parcel to cross the 5°-square. Thus, the computation still had a slight "memory" of the initial temperature in early 1972. The temperature was computed at ten points over the 5° of longitude in the box and these ten were averaged together to determine the mean monthly value. The values predicted by the model are shown in Fig. 7. The agreement between the observed and predicted curves is remarkably good. One might ask what the relative importance of local heating is compared to offshore advection. Shown also in this figure are the results of the computation when the model is purely advective, i.e., the local heating is set to zero. Obviously from November 1971 to March 1972 local heating plays a dominant role. This was especially true in early 1972 when the local winds and hence the offshore advection were weak. After April, offshore advection of coastal waters dominates. [This suggests that the normal seasonal cooling that starts in April (Fig. 3) is a result of enhanced offshore advection.] Thus, from April to November 1972, temperatures were anomalously high because the T_0's were high. This might have been the result of an abnormally deep thermocline along the coast which could have been produced by remote forcing (Enfield, 1980). To see what the effect of varying T_0 is, the mean-monthly temperatures from 1949 to 1977 along the coast were determined from data obtained from the National Climate Center. The difference between these values and those from the Ramage atlas is shown in Fig. 7. Apparently from February 1972 to February 1973 near-shore temperatures were about 2–4°C above the mean. After March 1973, the temperatures were almost normal. When these mean monthly values for T_0 were used in the model, the following occurred. The computed temperatures before April 1972 changed little. From April 1972 to April 1973 the computed temperatures were considerably lower, and the curve for 1972 looked like that for 1973. This supports the idea that the anomalously warm temperatures offshore of Peru in middle and late 1972 resulted from an increase in T_0, despite the fact that upwelling was going on. The computed temperatures in February and March 1972 were not much affected by the decrease in T_0 of ~2°C for these months because the offshore advection at this time was weak. In February the offshore advection was almost zero. In March, the residence time was still ten months. The strongest Q-anomalies, of the order of 50–100 W m^{-2}, as compared to 1973, occurred from November 1971 to March 1972. This

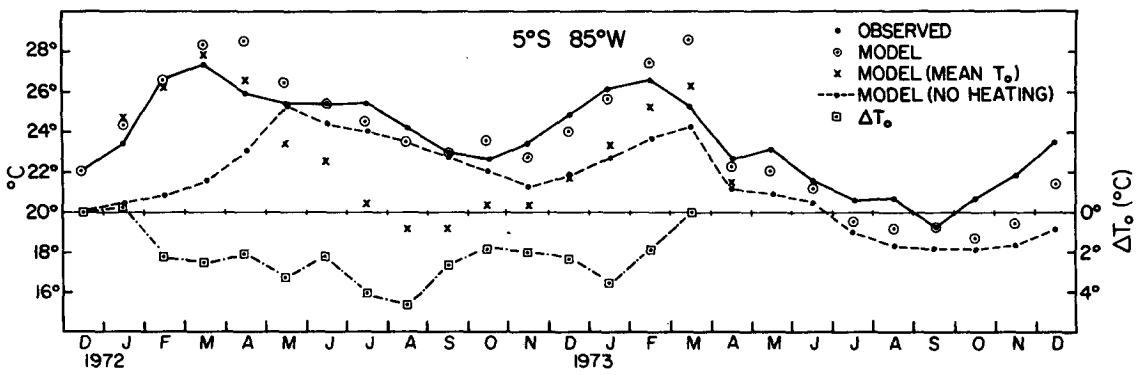

FIG. 7. Results of model computation.

anomalous heating, coupled with the seasonal heating at a time when the offshore advection was weak, produced the large temperature increase in early 1972. Whereas, the offshore advection of the warmer nearshore water maintains the higher temperatures offshore for the rest of the year.

5. Discussion

The following scenario is suggested. During the 1972–73 El Niño, from November 1971 to March 1972, the heating rates were larger than average. This resulted from increased local heating and reduced offshore advection of coastal waters. At the end of March, temperatures were anomalously high. With the onset of upwelling in April, normal or slightly greater than normal cooling took place. Abnormal cooling presumably resulted from increased evaporation which resulted from higher temperatures and higher wind speeds. However, because the nearshore waters that were advected offshore were themselves warmer than average, offshore temperatures remained anomalously high. The higher-than-average inshore temperatures could have been a result of a depressed thermocline next to the coast (Enfield, 1980). Without these higher inshore temperatures, the El Niño would have been short-lived since the residence time of the water offshore was only three to four months.

Thus, although local heating is important in annual and interannual temperature variations, it is not entirely clear if there are anomalous heat inputs into the ocean during *all* El Niños. These studies suggest that the local heating rates were greater than average in 1969 and 1972. Comparison of these computations with others such as those of Ramage *et al.* (1980) is difficult because the formulas and data sources are slightly different. Ramage's results, as was pointed out, also suggest that there was more heating of the ocean in 1972 than 1973.

However, it is hard to establish what the mean, or mean monthly heating rates are in this region. Ramage's two-year mean for the 5°-square at 5°S and 85°W is ~80 W m^{-2}. Hastenrath and Lamb (1977) get ~50 W m^{-2} for the same region, whereas Weare *et al.* (1981) get ~90 W m^{-2}. It is difficult to determine what is normal or anomalous unless such differences are resolved.

In February/March 1972 the near equatorial winds used in this computation weakened in phase with the normal seasonal cycle (Ramage *et al.*, 1980). This fact apparently contradicts the conclusion of Wyrtki (1975) that the winds off Peru are not weaker during El Niño. Wyrtki's conclusion was for yearly-averaged winds for the region 10–20°S and 70–80°W which lies farther south than the present region of interest. Also Enfield (1982) has pointed out that the nonseasonal variability is poorly correlated between coastal winds in the eastern Pacific and the oceanic winds farther offshore. Within 5° of the equator, Hickey (1975) found that the "El Niño phenomena . . . are clearly accompanied by a minimum of the zonal wind stress at most longitudes west of 120°W and in the meridional wind stress east of 120°W". In any case, because of the spatial and temporal variability in the winds, each specific region has to be examined individually and generalizations should be avoided.

APPENDIX

Local Heating Formulas

If a column of water with a unit horizontal cross section is considered, then the time rate of change of internal energy U, due to local heating is given by

$$\frac{dU}{dt} = Q_R - Q_B - Q_S - Q_E \text{ (cal cm}^{-2}\text{ s}^{-1}\text{)}, \quad (1)$$

where

Q_R short-wave radiation absorbed
Q_B net long-wave radiation emitted
Q_S sensible heat flux
Q_E evaporative heat flux.

The following bulk formulas were used to determine the fluxes in Eq. (1):

$$Q_R = Q_0[1 - (a + 0.38n)n](1 - \alpha), \quad (2a)$$

$$Q_B = [7.38 \times 10^{-3}(1 + 1.47 \times 10^{-2}T_s) \times (0.39 - 0.05e^{1/2})(1 - cn^2)], \quad (2b)$$

$$Q_S = 4.16 \times 10^{-7}(T_s - T_a)u, \quad (2c)$$

$$Q_E = 5.82 \times 10^{-4}p^{-1}[1.62(T_s - t') + 0.00066(1 + 0.00115t')p(T_a - t')]u, \quad (2d)$$

where

Q_0 shortwave radiation incident on earth's surface through a clear atmosphere [mean monthly values of Q_0 obtained from Berliand (1960)]
n fractional cloud cover
a coefficient (which ranged from 0.38–0.40 for the study area)
α albedo (0.06)
T_s sea surface temperature (°C)
e vapor pressure at ship level (mb)
c coefficient (which ranged from 0.50–0.55 for the study area)
T_a air temperature (°C)
t' wet bulb temperature (°C)
p barometric pressure (mb)
u wind speed (cm s^{-1}).

Eqs. (2a), (2b) and (2c) are essentially the same as Warren's (1972) Eqs., (2), (4) and (5), and are discussed in detail there. Eq. (2b) is in slightly different form than Warren's Eq. (4) due to the linearization scheme utilized by Warren to obtain his expression. To determine the vapor pressure e in Eq. (2c), the following equation from the *Smithsonian Meteorological Tables* (List, 1951) is used:

$$e = e' - [0.00066(1 + 0.00115t')p(T_a - t')], \quad (2e)$$

where e' is the saturated vapor pressure at temperature t'. Calculated values of e' over pure water were obtained from the *Smithsonian Meteorological Tables* (Table 94) for T_s ranging from 18 to 26°C and were then linearized by means of a linear regression to give the following expression

$$e' = 1.62T_s - 8.92 \text{ (mb)}, \quad (2f)$$

which has a maximum error of ~2% over the range considered. The effect of sea salt on vapor pressure is ignored.

The evaporative heat flux (Q_E) is generally written (Warren, 1972)

$$Q_E = KL(q_s - q_a)u, \quad (3)$$

where K is a constant, L is the latent heat of condensation of water vapor, q_s is the saturated specific humidity at T_s, and q_a is the specific humidity at T_a. Following the approximations of Byers (1944, p. 154),

$$q_s \approx 0.622p^{-1}[e'(T_s)], \quad q_a \approx 0.622[e(T_a)]p^{-1},$$

then using (2e) and (2f), the following equation can be derived

$$q_s(T_s) - q_a(T_a) \approx 0.622p^{-1}1.62(T_s - t') + 0.00066(1 + 0.00115t')p(T_a - t'). \quad (4)$$

Inserting Eq. (4) into (3) with $K = 1.6 \times 10^{-6}$ g cm^{-3} and $L = 585$ cal g^{-1}, Eq. (2d) is obtained.

REFERENCES

Berliand, T. G., 1960: Metodika klimatologicheskikn raschetov radiatsil. *Meteor. Gidrol.*, **6,** 9–16.

Byers, H. R., 1944: *General Meteorology,* 2nd ed. McGraw-Hill, 645 pp.

Bjerknes, J., 1966: Survey of El Niño 1957–58 in its relation to tropical Pacific meteorology. *Bull. Inter-American Tropical Tuna Commission,* **12,** No. 2, 25–86.

Busalacchi, A. J., and J. J. O'Brien, 1981: Interannual variability of the equatorial Pacific in the 1960's. *J. Geophys. Res.*, **86,** 901–907.

Dewitt, P. W., 1979: A local heating model of the monthly mean surface temperature fluctuations in the eastern tropical Pacific. (Unpublished manuscript.)

Enfield, D. B., 1980: El Niño–Pacific eastern boundary response to interannual forcing. *Resource Management and Environmental Uncertainty,* M. H. Glantz, Ed., 213–254.

——, 1983: Annual and non-seasonal variability of monthly low-level wind fields over the southeastern tropical Pacific. Submitted to *Mon. Wea. Rev.*

Hastenrath, S., and P. Lamb, 1977: *Climatic Atlas of the Tropical Atlantic and Eastern Pacific Oceans.* University of Wisconsin Press, 106 pp.

Hickey, B., 1975: The relationship between fluctuations in sea level, wind stress, and sea surface temperature in the equatorial Pacific. *J. Phys. Oceanogr.*, **5,** 460–475.

Horel, J. D., and J. M. Wallace, 1981: Planetary scale atmospheric phenomena associated with the southern oscillation. *Mon. Wea. Rev.*, **109,** 813–829.

Hoskins, B. J., and D. J. Karoly, 1981: The steady linear response of a spherical atmosphere to thermal and orographic forcing. *J. Atmos. Sci.*, **38,** 1179–1196.

List, R. J., 1951: *Smithsonian Meteorological Tables,* 6th ed. *Smithsonian Misc. Collect.*, 527 pp.

McCreary, J., 1976: Eastern tropical ocean response to changing wind systems: With application to El Niño. *J. Phys. Oceanogr.*, **6,** 632–645.

Ramage, C. S., C. W. Adams, A. M. Hori, B. J. Kilonsky and J. C. Sadler, 1980: *Meteorological Atlas of the 1972–1973 El Niño.* UH-MET 80-03, Dept. Meteor., University of Hawaii, Honolulu, 101 pp.

Rasmusson, E. M., and T. H. Carpenter, 1982: Variations in tropical sea surface temperature and surface wind fields associated with the Southern Oscillation/El Niño. *Mon. Wea. Rev.*, **10,** 354–384.

Sadler, J. C., L. Oda, and B. J. Kilonsky, 1976: Pacific Ocean cloudiness from satellite observations. UH-MET 76-01, Dept. Meteor. University of Hawaii, Honolulu, 137 pp.

Warren, B. A., 1972: Insensitivity of subtropical mode water characteristics to meteorological fluctuations. *Deep-Sea Res.*, **19,** 1–20.

Weare, B. C., P. T. Strub, and M. D. Samuel, 1981: Annual mean surface heat fluxes in the tropical Pacific Ocean. *J. Phys. Oceanogr.*, **11,** 705–717.

Wyrtki, K., 1964: The thermal structure of the eastern Pacific Ocean. *Dtsch. Hydrogr. Z.*, **A6,** 84 pp.

——, 1975: El Niño: The dynamic response of the equatorial Pacific Ocean to atmospheric forcing. *J. Phys. Oceanogr.*, **5,** 572–584.